BASIT ET AL (2023), *FUUAST J.BIOL.*, 13(1): 27-37

COMPARING RADIATIVE TRANSFER EQUATION METHOD (RTEM) AND THE GENERALIZED SINGLE-CHANNEL METHOD (GSCM)FOR RETRIEVING SEA SURFACE TEMPERATURE ALONG THE KARACHI COAST, PAKISTAN.

ABDUL BASIT[1], RAO ZAHID KHALIL[1], IMRAN AHMED KHAN[3], IBRAHIM ZIA[2], SADAF SADIQ[1] AND SAJID MAJEED[1]

[1]Institute of Space Technology, Islamabad, Pakistan
[2]National Institute of Oceanography, Karachi, Pakistan
[3]Department of Geography, University of Karachi, Karachi, Pakistan
Corresponding author`s email: ab.basit93@gmail.com

خلاصہ

سمندری سطح کے درجہ حرارت کی نگرانی (SST) آبی ماحولیاتی نظام میں مختلف عملوں کے اثرات کو سمجھنے کے لیے بہت ضروری ہے۔ کراچی، پاکستان کا ساحلی پانی خاص طور پر صنعتوں اور پاور پلانٹس سے ہونے والی آلودگی سے متاثر ہے سطحی سمندری درجہ حرارت کو مؤثر طریقے سے نگرانی کرنے اور تبدیلیوں کا پتہ لگانے کے لئے، سیٹلائٹ ریموٹ سینسنگ کو مستقل اور قابل اطمینان طریقہ تصور کیا گیا ہے۔ یہ مطالعہ ایس ایس ٹی کا تخمینہ لگانے کے دو طریقوں کی کارکردگی کا موازنہ کرتا ہے، ریڈی ایٹیو ٹرانسفر ایکویشن میتھڈ (RTEM) اور جنرلائزڈ سنگل چینل میتھڈ (GSCM) ۔ رجحانات کا تجزیہ کرنے کے لیے باہمی ربط اور لینئیر ریگریشن ماڈلز کا اطلاق کیا گیا، اور لینڈ سیٹ ای ٹی ایم + تھرمل انفرا ریڈ ڈیٹا کا استعمال کرتے ہوئے ایک طرفہ انووا کی بھی گنتی کی گئی۔ ایس ایس ٹی کے تخمینے 14 مختلف مقامات پر ان سیٹو ڈیٹا اور ایک سمپل ریگریشن تکنیک کا استعمال کرتے ہوئے حاصل کیے گئے تھے۔ نتائج سے ظاہر ہوتا ہے کہ دونوں طریقوں کا ان سیٹو پیمائش کے ساتھ انتہائی اہم تعلق ہے، جس میں RTEM کے لیے 0.51 اور GSCM کے لیے بالترتیب 0.80 کے گتانک (R2) کے ساتھ۔ دونوں طریقوں میں قابل قبول معیاری غلطیاں بھی ہیں، جس میں GSCM کا RMS 1.50 ہے اور RTEM کا RMS 2.40 ہے۔ عام طور پر، حقیقی زمینی ڈیٹا کا استعمال کرتے وقت دونوں نقطہ نظر ایک مضبوط شماریاتی رجحان دکھاتے ہیں.

Abstract

The monitoring of sea surface temperature (SST) is crucial for understanding the impact of various processes in aquatic ecosystems. The coastal waters of Karachi, Pakistan are particularly affected by pollution from industries and power plants. To effectively monitor and detect changes in SST, satellite remote sensing has been proposed as an efficient and cost-effective method. This study compares the performance of two methods for estimating SST, the Radiative Transfer Equation Method (RTEM) and the Generalized Single-Channel Method (GSCM). Correlation and linear regression models were applied to analyze trends, and a one-way ANOVA was also computed using Landsat ETM+ thermal infrared data. SST estimates were obtained at 14 different locations using in-situ data and a simple regression technique. The results indicate that both methods have a highly significant relationship with in-situ measurements, with the coefficient of determination (R2) of 0.51 for RTEM and 0.80 for GSCM, respectively. Both methods also have acceptable standard errors, with GSCM having an RMS of 1.50 and RTEM having an RMS of 2.40. In general, both approaches show a strong statistical trend when using real-ground data.

Keywords: Sea Surface Temperature, Radiative Transfer Equation, Generalized Single Channel Method, Landsat ETM +, Digital Numbers GLM.

Introduction

The temperature of the sea surface, or SST, is a critical aspect of the energy exchange between the water and atmosphere and is therefore a vital characteristic of aquatic systems. It plays a significant role in regulating many natural and chemical processes in the aquatic environment. To effectively understand the functioning of oceans, lakes, and reservoirs and manage water quality, land use, and hydrological research, it is necessary to monitor the distribution of SST. Studies have shown the importance of SST in water resource management (Threlkeld, 1990; Kay *et al*., 2005).

The conventional methods of examining sea surface temperature (SST) through field surveys are costly, time-consuming, and often not very precise. Advancements in remote sensing techniques have provided cost-effective alternatives for monitoring and detecting geophysical parameters (Schneider and Mauser, 1996; Thiemann and Schiller, 2003). Remote sensing offers efficient and comprehensive coverage and provides additional and crucial detail from the non-visible regions of the electromagnetic spectrum (Sprint *et al*., 2002;

de Moraes Novo *et al*., 2006; Alcantara *et al*., 2009). Water quality parameters in ocean environments are usually detected based on the characteristics of the water and the sensor used, with a good spatial and temporal resolution. Satellites with radiometric, spectral, and temporal resolution are now more frequently used (Giardino *et al*., 2001; Lamaro *et al*., 2013; Dekker and Peters 1993; Schneider and Mauser 1996). The energy interactions between the atmosphere and water mass generally occur within the very thin surface, i.e., top layer that is sensed by satellite remote sensing. Factors such as wind speed, *evaporative* cooling, and energy changes due to diurnal variation make the phenomena complex. However, some studies (Yokoyama, Tanba, and Souma 1995; Schneider and Mauser 1996) have shown that skin temperature can be used as a proxy for water temperature.

The surface temperature of the water can be quantified by measuring the emitted radiation of thermal infrared (TIR) with a wavelength of 8-14 micrometers (μm) (Donlon *et al*., 2002; Kay *et al*., 2005). However, these measurements need to be atmospherically corrected in a quantitative manner (Li *et al*., 2013) to account for the effects of the atmosphere on the temperature readings. The recovered temperatures are assumed to be the same for all thermal band sensors, but differences in temperature among bands can occur due to issues with atmospheric correction (generally, the correction is found to be good at bands of wavelength around 10-11 μm and poor for around 12 μm bands).

In recent years, there has been a significant improvement in the calibration methodologies for interpreting thermal infrared images, thanks to rapid advancements in technology. Studies have been conducted using these data to map sea surface temperature (SST), particularly in areas that exhibit obvious variations such as near nuclear plants and hot springs (Gibbons *et al*., 1989).

The surface temperature can be estimated from surface emissivity and at-sensor data using a variety of approaches, particularly for land. For Landsat bands, there are two ways to rectify a single thermal band, the thermal infrared band. One approach is to use the Radiative Transfer Equation (RTE) methods (Hook *et al*., 2004). These techniques employ radiative transfer modeling software to calculate the atmosphere's transmissivity, down welling, and upwelling radiance. Another option is to use single-channel algorithms that also rely on RTE approximations. These methods, despite their reduced precision, minimize the need for in-situ radio-sounding data, making them suitable for archive studies. Jiménez-Muoz and Sobrino developed the Generalized Single-Channel technique in 2003, which uses water vapor content as secondary data. With known sensor emissivity, this method only requires the effective wavelength of the sensor, at-sensor data (at-sensor radiance or brightness temperature), and the total water vapor content of the atmosphere (Sobrino, Jiménez-Muoz, and Paolini, 2004)

Coastal waters of Pakistan along Karachi are very severely affected due to various sources of pollution, such as industry and power plants. It also creates thermal pollution which lowers and increases dissolved oxygen and respiration rates respectively, resulting in aquatic life being in danger. This study is an effort to assess the temperature of coastal water in some critical locations such as the Malir and Lyari River outfalls, Karachi harbor, and Gizri Creek. In this study, an attempt has been made to explore the applicability of two existing surface temperature algorithms (Single Channel and Radiative Transfer) to retrieve SST in Karachi coastal water using Landsat ETM+ thermal infrared data.

Material and Methods

Study area: Karachi coast between the outfalls of Lyari and Malir Rivers including Karachi harbor and Gizzri Creek has been selected for the study (Figure1). Karachi port is among the largest and the busiest deep-water ports in South Asia. The pollution induced by port activities can be expected to impact the quality of water. The harbor is located between the Karachi towns of Kimari and Saddar, and due to its proximity to many industrial areas, the waste generated from these areas also impacts its water quality. The main contributors of industrial waste are the Malir and Lyari rivers, which have been converted into waste drains in recent years.

Methodology: In this study, Landsat TM, ETM+, and TIRS sensors were used for the years 2002, 2013-14, and 2018, respectively, for this, one thermal infrared image was taken for each year from the USGS (United States of Geological Survey https:/earthexplorer.usgs.gov). The selection of images was within the criteria of ± 3 days of the in-situ data. The data consists of 14 different locations along the coastal region of Karachi as shown in Figure (1). Extraction of pure water pixels and elimination of pixels that are not characteristic of open water is important to avoid any discrepancy in the SST values along the study area. To select pure water pixels and eliminate land pixels, the Normalized Difference Water Index (NDWI) is used to extract water pixels using appropriate thresholding.

To calculate SST, a low gain thermal band is used for this purpose, since it is not saturated, and the range is greater than a high gain thermal band. The overall methodological framework is as Figure (2). The conversion of digital numbers (DN) of the thermal band to a physical variable such as radiance and reflectance is essential to make it meaningful for interpretation and to compare it with other data. To do so two main steps are required, i.e., the radiometric and atmospheric corrections. By applying equation 1, the radiometric correction was done

which converts the values of DN to at-sensor uncorrected spectral radiance (Lλ) in W.m^{2}sr. µm. Where Q_{Cal} is pixel a value in DN; Q_{Calmax}, Q_{calmin}, L_{max}, L_{min}, are the constants given in Land sat data user's handbook.
The output derived from Equation 1 was converted to at-sensor brightness temperature (T_b) in Kelvin using Equation 2 which is relied on Planck's law (Wukelic *et al*., 1989).

$$L_\lambda = \frac{(L_{max} - L_{min})}{QCal_{max} - QCal_{min}} \times (QCal - QCal_{min}) + L_{min} \quad (1)$$

$$T_b = \frac{K_2}{ln\left(\frac{K_1}{L_\lambda} + 1\right)} \quad (2)$$

where K_1 and K_2 are the constants of the thermal band retrieved from the file of metadata provided in the data set.

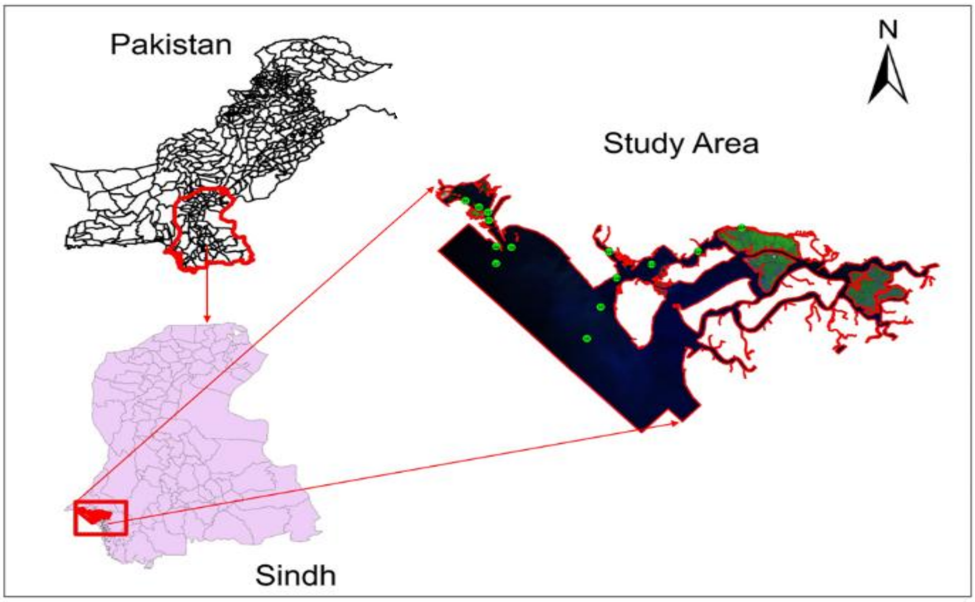

Fig. 1. Study Area of Lyari and Malir Rivers including Karachi harbor and Gizzri Creek

Methods for SST Estimation

Radiative transfer equation method (RTEM)

The atmospheric conditions can affect the received signals up to 90% for water bodies, which can change the SST values up to ±20^{0}C (Kay *et al*. 2005) when constant emissivity is used for water. As the thermal band is not atmospherically corrected, a correction was made to retrieve the corrected water surface radiance (Lλ(Ts)) using equation (3), as done by Srivastava *et al*. It requires uncorrected spectral radiance (Lλ) calculated from Equation (1), upward radiance (Lλup), downward radiance (Lλdown), atmospheric transmissivity (τ), and water surface emissivity (ε). The invariable value of 0.98 for water emissivity, as suggested by (Snyder *et al*. 1998), was used in this study. The atmospheric correction parameter calculator was used to obtain such atmospheric parameters (Lλup, Lλdown, and τ), developed by (Barsi, Barker, and Schott, 2003) which uses the MODTRAN simulator.

Equation 4 shows how to convert corrected water surface radiance (Lλ (Ts)) to Land surface temperature (LST) utilizing the relationship with the plan equation with two thermal constants K1 and K2. (Sinha *et al*. 2014; Srivastava, Majumdar, and Bhattacharya 2009).

$$L_{\lambda(Ts)} = \frac{L_\lambda - L_{\lambda up}}{\{\tau \times \varepsilon\}} - \frac{1-\varepsilon}{\varepsilon} \times L_{\lambda down} \quad (3)$$

$$T_s = \frac{K_2}{ln\left(\frac{K_1}{L_{\lambda(Ts)}} + 1\right)} \quad (4)$$

where, Ts = surface temperature; Lλ(Ts)= corrected surface radiance, and K1 and K2 are the thermal constants.

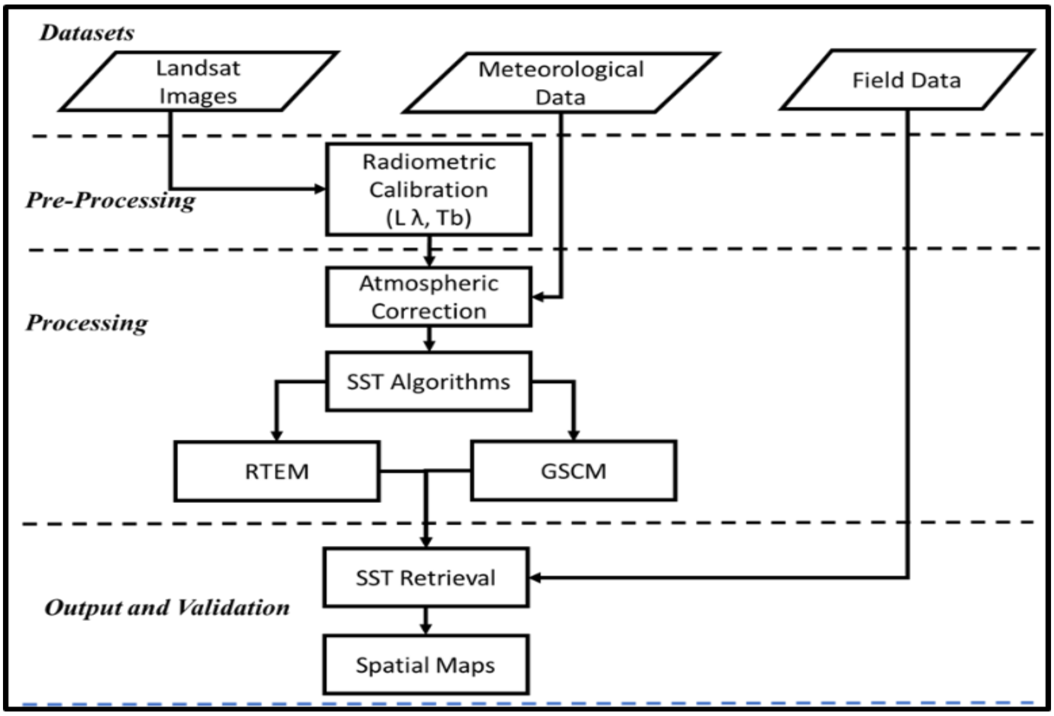

Fig.2. Flow Chart for the retrieval of Sea Surface Temperature from RTEM and GSCM

Generalized Single Channel Method (GSCM)

This algorithm (Jiménez-Muñoz and Sobrino 2003) was developed to retrieve surface temperature using a single thermal infrared band. Following are the equations (5)-(7) which can be used to retrieve surface temperature.

$$T_s = \gamma[\, \varepsilon^{-1}(\psi_1 L_\lambda + \psi_2) + \psi_3 + \delta \quad (5)$$

$$\gamma = \{\frac{C_2 L_\lambda}{T_b^2}\left[\frac{\lambda^4}{C_1} L_\lambda + \lambda^{-1}\right]\}^{-1} \quad (6)$$

$$\delta = -\gamma L_\lambda + T_b \quad (7)$$

$$\psi_1 = 0.14714\omega^2 - 0.15583\omega + 1.1234 \quad (8)$$

$$\psi_2 = -1.1836\omega^2 - 0.3760\omega - 0.52894 \quad (9)$$

$$\psi_3 = -0.04554\omega^2 + 1.8719\omega - 0.39071 \quad (10)$$

$$\omega = 0.0981 \times \left\{10 \times 0.6108 \times exp\left[\frac{17.27 \times (T_0 - 273.15)}{237.3 \times (T_0 - 273.15)}\right] \times RH\right\} + 0.1679 \quad (11)$$

Where the surface temperature Ts is in Kelvin, λ stands for effective wavelength which is 11.45 μm, ε is the water surface emissivity (0.98), γ and $\delta$are the Planck's function-dependent parameters, C_1= 1.19104 x 108

$W\mu m^4.m^{-2}.sr^{-1}$, C_2= 14387.7 µm. K, Lλ, and Tb are calculated in Equations (1) and (2), respectively. The Ψ1, Ψ2, and Ψ3 are the atmospheric functions calculated using the following equations (8)-(10), respectively. These atmospheric functions require the content of water vapor (ω) in the atmosphere during the overpass time of the satellite. The estimation of atmospheric water vapor equation (11) (Yang, Sinica, and 1996, n.d.; Liu *et al*. 2011) can be used which only requires air temperature near the surface (T_0) in Kelvin and relative humidity (RH).

Trend Analysis with GLM and One-way ANOVA

The Generalized Linear Model (GLM) and one-way Analysis of Variance (ANOVA) trend analysis were employed to evaluate the trend of the estimated points obtained from the Generalized Single-Channel Method (GSCM) and the Radiative Transfer Equation Method (RTEM) with in-situ data. GLM is a statistical technique that is used to measure the correlation among data sets and assess the effectiveness of treatment over time. It is commonly used with categorical or continuous data as independent variables and can be used to examine the primary effects within and between subjects, interaction effects between variables, the effects of covariates, and the effects of interactions between covariates and factors between subjects. One-way ANOVA is a statistical method used to determine whether there are any significant differences between the means of two or more independent groups. It is often used when there are at least three groups, rather than just two. The method is used to determine whether there are any statistically significant differences between the means of the groups being compared.

Results and Discussion

Estimated values of SST were obtained by the two compared methods RTEM and GSCM which were correlated by applying a simple linear regression model. The R-squares for RTEM and GSCM were 0.51 and 0.81 and RMSE were 2.40 and 1.53, respectively. The GSCM method shows a very good adjustment with in-situ measurements, although RTEM did not show a good adjustment within situ measurements in which they had a low coefficient of relation while their standard errors were also high, as shown in Table (1). Scatter plots were also drawn for each method against in-situ measurements as shown in Figure (3).

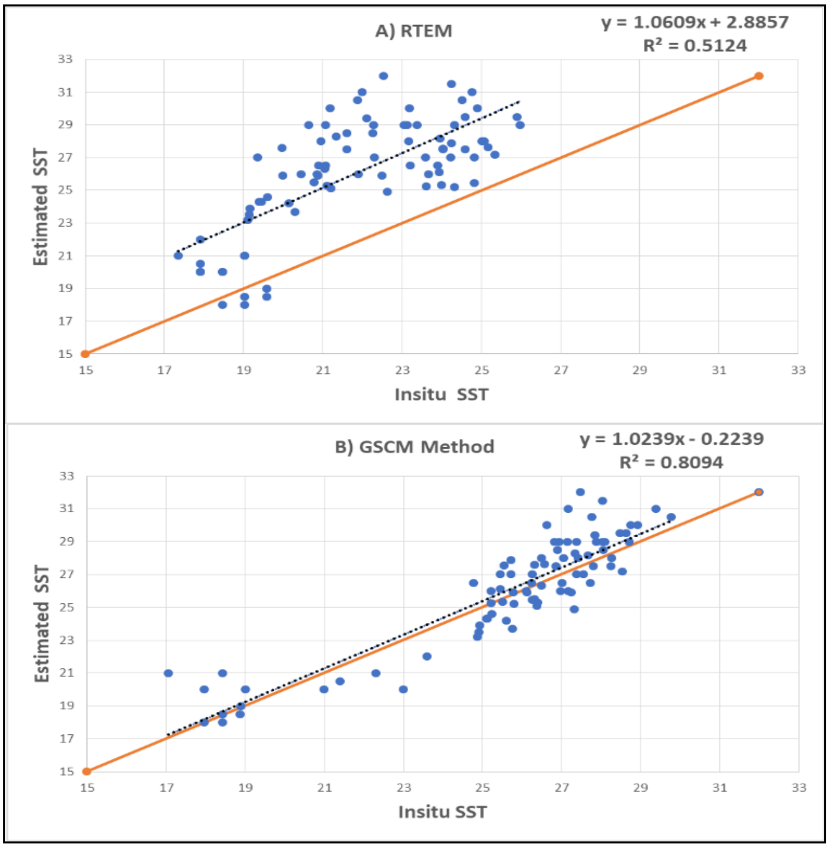

Fig.3. Scatter Plot between measured SST(Celsius) and Observed SST A) Radiative Transfer Equation Method (RTEM) B) Generalized Single Channel Method (GSCM).

Figure (4) shows data in time series, this type of plot allows us to highlight the accuracy of both methods. The SST values estimated by RTEM were lower than those for the GSCM, but they also showed a trend with in-situ measurements. Both methods almost underestimated in-situ values, except in the case of September 2013 GSCM method overestimated in-situ values. This situation occurs due to seasonal variation or because these stations were placed near the outfalls of the Karachi megacity.

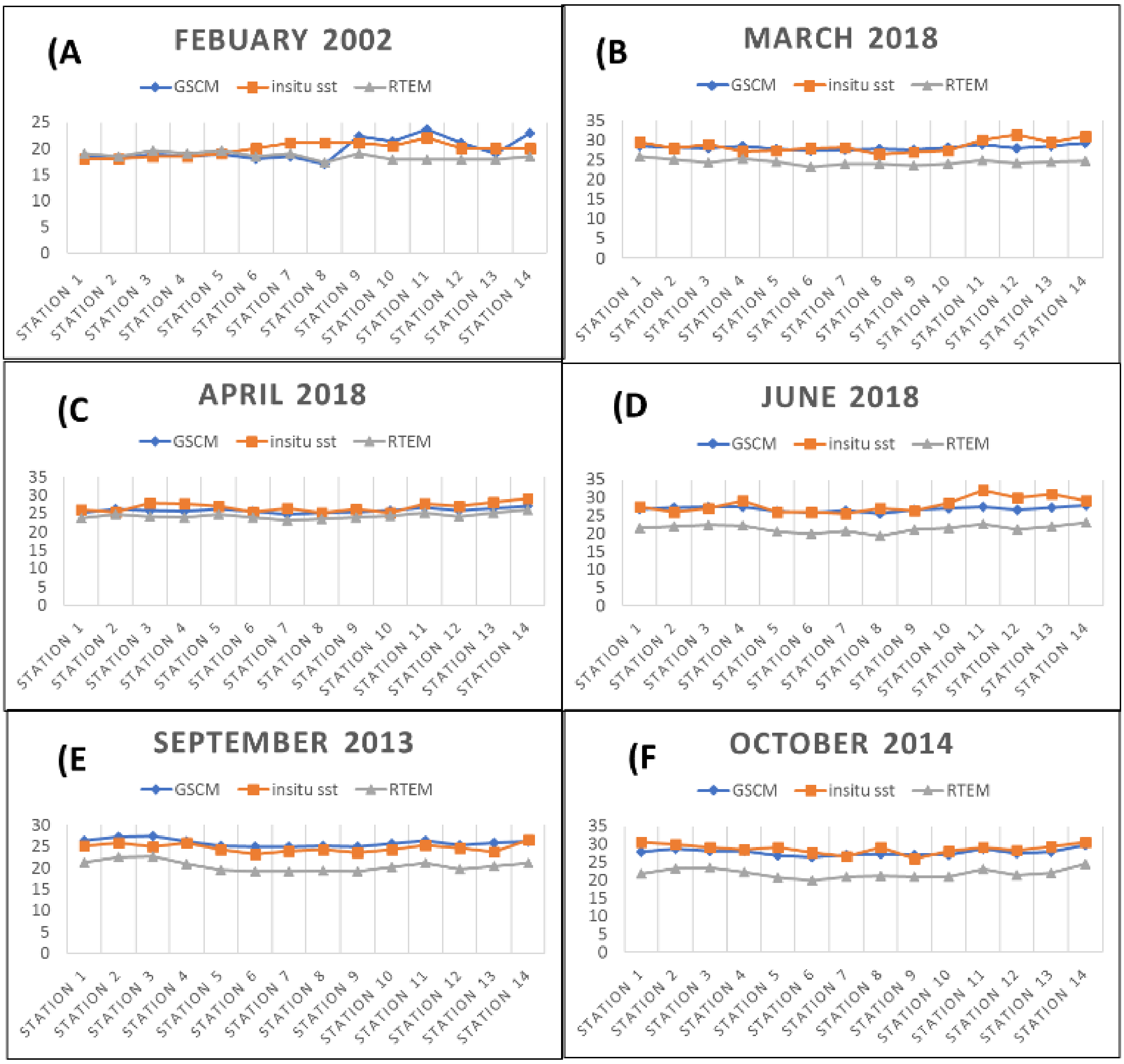

Fig.4. Comparison of measured and observed SST (Celsius) on Y-axis with RTEM and GSCM method over sampling stations.

Trend Analysis

GLM Measures

Estimated points from GSCM and RTEM with in-situ measurement showed statistically significant $p<0.05$, Sum of Square 6.353 and 746.232 respectively. Other parameters also showed a linear trend between them as shown in Table (2). Figure (7) and Figure (8) also show the linear trend between in-situ and estimated data.

One-way ANOVA

Estimated points from GSCM and RTEM with in-situ measurement having $p<0.05$, Sum of Square 606.6 and 226.45, and other parameters values showed the linear trend between them as shown in Table (3). Figure (9) showed the GSCM trend line increasing linearly which showed a good trend between the estimated value of GSCM and in-situ measurements. But in the case of Figure (10), the RTEM linear trend line was not good as compared to the GSCM trend line.

Spatial distribution of SST

We produced the SST maps based on the GSCM Figure (5, 6) considering the obtained results, and that GSCM uses simple data for atmospheric correction and makes its application possible for the different thermal sensors.

Validation

From 84 in situ measurements the validation was checked using simple regression analysis between estimated SST values from RTEM and GSCM methods and in situ SST values. In addition, the quality of results was also checked between estimated and in situ values using categorical statistics e.g., RMSE, Standard deviation, Coefficient of relation, Sig. F Change, Adjusted R Square, R Square Change, F Change.

Table 1. Regression analysis of the comparison between estimated and measured SST for both methods.

Model	R	R square	Adjusted R square	N	Std. The error of the estimate	Change statistics		
						R square change	F change	Sig. F change
GSCM	.900	.809	.807	84	1.50211	0.809	348.196	.000
RTEM	.716	.512	.506	84	84	0.512	86.170	.000

Table 2. Trend line analysis of GLM method

M		Sum of square	F	Sig.
GSCM	Linear	6.353	5.687	<0.05
RTEM	Linear	746.232	260.826	<0.05

Table 3. Trend line analysis of One-way ANOVA method

One Way-ANOVA		Sum of squares	F	Sig.
GSCM	Linear	606.584	411.44	<0.05
RTEM	Linear	226.448	95.658	<0.05

Specific number and field examples such as global climate change, hydrological, geo-/biophysical, and urban land use/land cover, rely heavily on LST. LANDSAT 8, the most recent satellite in the LANDSAT family to be launched, has opened new opportunities for using remote sensing to better understand Earth's occurrences. A new procedure-based technique for automatically mapping LST from LANDSAT 8 data is presented in this paper. Environmental data is a critical component of human health research, and remote sensing is a widely used method for obtaining it. Temperature can be calculated from remote sensing data by computing LST, which is the temperature felt at ground level. This is a topic of such scholarly interest that various research on computing LST from diverse sources and using various techniques has been published. Several academics, for example, have examined several algorithms to find the most accurate one, either by adjusting the computation's inputs or the approach used.

It is imperative to keep in mind that in 2009 the single-channel framework was reexamined in this examination (Jiménez-Muñoz *et al*., 2009), and they upgraded the coefficient's included within the relationship between climatic work (w1, w2, and w3) and air-water vapor (w) for Landsat 5 TM, Landsat 4 and Landsat 7 ETM+ comes about. Five isolated barometrical sounding databases were considered to deliver mimicked information and confirm the calculation. Although we have not connected this examination in this work, we compared the RMS values gotten and drift investigation between in situ and evaluated information. The connection with the in-situ information of our values is based on RMS = 1.50211, which is suitable relative to the values gotten by Jiménez-Muñoz *et al*. (2009) conjointly the slant for both models was direct, decently great, and worthy. On the other hand, in 2010 the same creators connected the same calculation with amazing comes with ASTER data (Jiménez-Muñoz and Sobrino, 2010).

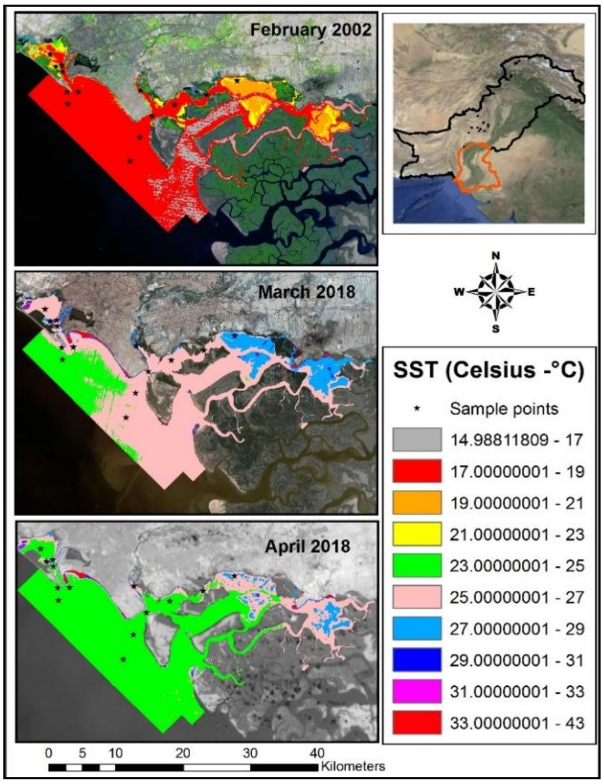

Fig. 5. SST Maps for February 2002, March 2018, and April 2018

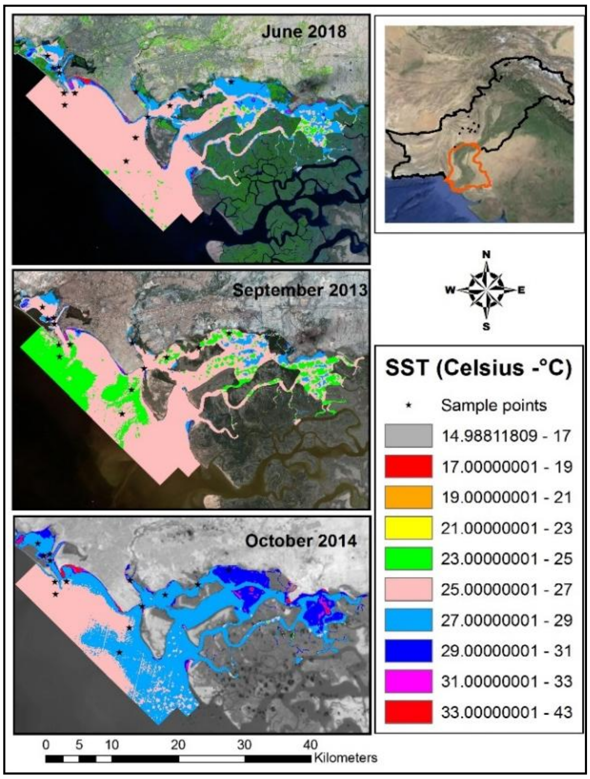

Fig. 6. SST Maps for June 2018, September 2013, and October 2014

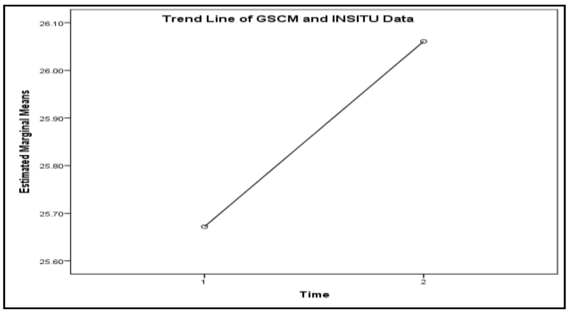

Fig. 7. GLM method linear trend line graph of GSCM and in-situ data

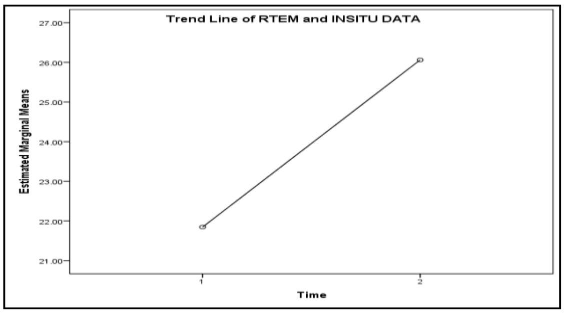

Fig. 8. GLM method linear trend line graph of RTEM and Insitu data

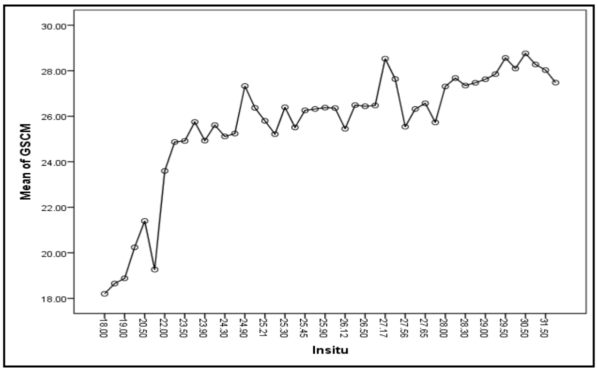

Fig. 9. One Way ANOVA Linear Trend Line Graph of GSCM and Insitu data

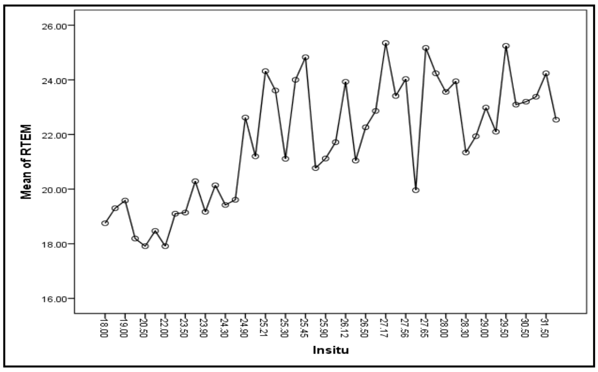

Fig. 10. One Way ANOVA Linear Trend Line Graph of RTEM and In-situ data

Conclusion

This study evaluated the use of two methods, the Generalized Single-Channel Method (GSCM) and the Radiative Transfer Equation Method (RTEM), for determining the sea surface temperature (SST) in the Karachi Harbor and Gizzri Creek. The GSCM method was found to be more effective in measuring minor temperature differences using in-situ data. Therefore, we conclude that the GSCM method is the best tool for monitoring SST in this region when using satellite imagery. Additionally, one of the advantages of this method is that it only requires the value of ambient water vapor, which is easy to collect and can be applied to other thermal sensors using the same coefficients and equations.

Acknowledgment

We would like to express our gratitude to the National Institute of Oceanography for providing the data used in this study. Their contribution was essential to the success of this research project, and we appreciate their willingness to share their resources.

We would also like to thank our research participants for their time and effort in participating in this study. Their insights and experiences were invaluable in helping us understand the phenomenon under investigation. Furthermore, we would like to thank our colleagues who provided support and assistance throughout the research process. Their feedback and guidance were instrumental in shaping our ideas and refining our methods.

References

Alcíntara, Enner, Cláudio Barbosa, José Stech, Evlyn Novo, and Yosio Shimabukuro. (2009). "Improving the Spectral Unmixing Algorithm to Map Water Turbidity Distributions" Environmental Modelling & Software 24 (9): 1051–61. https://doi.org/10.1016/J.ENVSOFT.2009.02.013.

Alcantara, C., Domingues, R. and Silva, E. (2009). A comparison of sea surface temperature retrieval methods using AVHRR data. International Journal of Remote Sensing, 30(12), 3129-3139.

Barsi, Julia, A., John, L., Barker, and John R Schott. (2003). "An Atmospheric Correction Parameter Calculator for a Single Thermal Band Earth-Sensing Instrument."

Barton, I. J., Satellite-derived sea surface temperatures: A comparison between operational, theoretical and experimental algorithms, J. Appl. Meteorol., 31, 432–442, 1992.

Barton, I. J. (1983). Dual-channel satellite measurements of sea surface temperature. Quarterly Journal of the Royal Meteorological Society, 109(460), 365-378.

Dash, P., F.-M. Göttsche, F.-S. Olesen, and H. Fischer. 2002. "Land Surface Temperature and Emissivity Estimation from Passive Sensor Data: Theory and Practice-Current Trends." International Journal of Remote Sensing 23 (13): 2563–94. https://doi.org/10.1080/01431160110115041

Dash, P., F.-M. Göttsche, F.-S. Olesen, and Fischer, H. Land surface temperature and emissivity estimation from passive sensor data: Theory and practice-current trends, Int. J. Remote Sens., 23, 2563–2594, 2002.

De Moraes Novo, E., Chaves, P. and Silva, E. (2006). Sea surface temperature retrieval from AVHRR and MODIS data using artificial neural networks. Journal of Marine Systems, 58(1-2), 49-61.

Dekker, A. G. and Peters, S. W. M. (1993). "The Use of the Thematic Mapper for the Analysis of Eutrophic Lakes: A Case Study in the Netherlands." International Journal of Remote Sensing 14 (5): 799–821. https://doi.org/10.1080/01431169308904379.

Dekker, A. and Peters, J. (1993). Remote sensing of ocean colour: An overview of the state of the art. Journal of Marine Systems, 4(1-2), 1-21.

Donlon, C. J., Minnett, P. J., Gentemann, C., Nightingale, T. J., Barton, I. J., Ward, B. and Murray. M. J. (2002). "Toward Improved Validation of Satellite Sea Surface Skin Temperature Measurements for Climate Research." Journal of Climate 15 (4): 353–69. https://doi.org/10.1175/1520-0442(2002).

Donlon, C. J., Minnett, P. J., Gentemann, C. L. and Wick, G. A. (2002). Towards the validation of high accuracy, global sea surface temperature measurements from the advanced along-track scanning radiometer. Journal of Geophysical Research: Oceans, 107(C6), 3-1.

Giardino, Claudia, Monica Pepe, Pietro Alessandro Brivio, Paolo Ghezzi, and Eugenio Zilioli. (2001). "Detecting Chlorophyll, Secchi Disk Depth and Surface Temperature in a Sub-Alpine Lake Using Landsat Imagery." Science of The Total Environment 268 (1–3): 19–29. https://doi.org/10.1016/S0048-9697(00)00692-6.

Giardino, C., Santoleri, R. and Mazzarella, A. (2001). Sea surface temperature retrieval from AVHRR data: A comparison of different algorithms. International Journal of Remote Sensing, 22(2), 225-235.

Gibbons, D. E., Wukelic, G. E., Leighton, J. P. and Doyle. M. J. (1989). "Application of Landsat Thematic Mapper Data for Coastal Thermal Plume Analysis at Diablo Canyon," June.

Gibbons, W. and Rottman, J. (1989). Temperature measurements of the Earth's surface by satellite-borne infrared sensors. Remote sensing of environment, 27(3), 263-270.

Hook, S. J., Chander, G. Barsi, J.A., Alley, R.E., Abtahi, A., Palluconi, F. D., Markham, B. L. Richards, R. C., Schladow, S. G. and Helder. D. L. (2004). "In-Flight Validation and Recovery of Water Surface Temperature with Landsat-5 Thermal Infrared Data Using an Automated High-Altitude Lake Validation Site at Lake Tahoe." IEEE Transactions on Geoscience and Remote Sensing 42 (12): 2767–76. https://doi.org/10.1109/TGRS.2004.839092.

Hook, S. J., Friedl, M. A. and Widlowski, J. L. (2004). A review of current and emerging techniques for retrieving land surface temperature from remote sensing data. Remote sensing of environment, 90(4), 354-383.

Jiménez-Muñoz, Juan C. and José A. Sobrino. (2003). "A Generalized Single-Channel Method for Retrieving Land Surface Temperature from Remote Sensing Data." *Journal of Geophysical Research* 108 (D22): 4688. https://doi.org/10.1029/2003JD003480.

Jiménez-Muñoz, J. C. and Sobrino, J. A. (2003). A generalized single-channel method for retrieving land surface temperature from remote sensing data. Journal of Geophysical Research: Atmospheres, 108 (D22).

Kay, Jennifer E., Stephanie, K., Kampf, Rebecca N. Handcock, Keith A. Cherkauer, Alan R. Gillespie, and Stephen J. Burges. (2005). "Accuracy Of Lake and Stream Temperatures Estimated from Thermal Infrared Images." Journal of the American Water Resources *Association* 41 (5): 1161–75. https://doi.org/10.1111/j.1752-1688.2005.tb03791.x.

Kay, J. E. and Gao, B. C. (2005). Thermal infrared remote sensing of sea surface temperature. Progress in Physical Geography, 29(4), 503-527.

Lamaro, Anabel Alejandra, Alejandro Mariñelarena, Sandra Edith Torrusio, and Silvia Estela Sala. (2013). "Water Surface Temperature Estimation from Landsat 7 ETM+ Thermal Infrared Data Using the Generalized Single-Channel Method: Case Study of Embalse Del Río Tercero (Córdoba, Argentina)." Advances in Space Research 51 (3): 492–500. https://doi.org/10.1016/J.ASR.2012.09.032.

Lamaro, M., Guarnieri, A. and Santoleri, R. (2013). Retrieval of sea surface temperature from MODIS-Terra and Aqua data: A comparison of different algorithms. Journal of Marine Systems, 119, 136-145.

Lagouarde, J. P., Kerr, Y. H., and Brunet, Y. An experimental study of angular effects on surface temperature for various plant canopies and bare soils, Agric. Forest Meteorol., 77, 167–190, 1995.

Li, Zhao-Liang, Bo-Hui Tang, Hua Wu, Huazhong Ren, Guangjian Yan, Zhengming Wan, Isabel F. Trigo, and José A. Sobrino. 2013. "Satellite-Derived Land Surface Temperature: Current Status and Perspectives." Remote Sensing of Environment 131 (April): 14–37. https://doi.org/10.1016/J.RSE.2012.12.008.

Liu, Lin, Yuanzhi Zhang, Lin Liu, and Yuanzhi Zhang. (2011). "Urban Heat Island Analysis Using the Landsat TM Data and ASTER Data: A Case Study in Hong Kong." *Remote Sensing* 3 (7): 1535–52. https://doi.org/10.3390/rs3071535.

Li, X., Liang, S. and Zhang, Y. (2013). A review on atmospheric correction of satellite ocean color data. Journal of Geophysical Research: Oceans, 118(9), 4305-4326.

Moraes Novo, Evlyn Márcia Leão de, Cláudio Clemente de Farias Barbosa, Ramon Moraes de Freitas, Yosio Edimir Shimabukuro, John M. Melack, and Waterloo Pereira Filho. 2006. "Seasonal Changes in Chlorophyll Distributions in Amazon Floodplain Lakes Derived from MODIS Images." *Limnology* 7 (3): 153–61. https://doi.org/10.1007/s10201-006-0179-8.

Qin, Z., Karnieli, A. and Berliner, P. A mono-window algorithm for retrieving land surface temperature from Landsat TM data and its application to the Israel-Egypt border region, Int. J. Remote Sens., 22, 3719–3746, 2001.

Schneider, K. and Mauser. W. (1996). "Processing and Accuracy of Landsat Thematic Mapper Data for Lake Surface Temperature Measurement." *International Journal of Remote Sensing* 17 (11): 2027–41. https://doi.org/10.1080/01431169608948757.

Schneider, W. and Mauser, W. (1996). Remote sensing of ocean surface temperature by means of passive microwave measurements. Journal of Geophysical Research, 101(C2), 3913-3924.

Schmugge, T., French, A., Ritchie, J. C., Rango, A. and Pelgrum, H. Temperature and emissivity separation from multispectral thermal infrared observations, Remote Sens. Environ., 79, 189–198, 2002.

Sinha, Suman, Prem Chandra Pandey, Laxmi Kant Sharma, Mahendra Singh Nathawat, Pavan Kumar, and Shruti Kanga. 2014. "Remote Estimation of Land Surface Temperature for Different LULC Features of a Moist Deciduous Tropical Forest Region." I, 57–68. https://doi.org/10.1007/978-3-319-05906-8_4.

Snyder, W. C., Wan, Z. Zhang, Y. and Feng. Y.-Z. (1998). "Classification-Based Emissivity for Land Surface Temperature Measurement from Space." *International Journal of Remote Sensing* 19 (14): 2753–74. https://doi.org/10.1080/014311698214497.

Sobrino, José A., Juan, C.. Jiménez-Muñoz, and Leonardo Paolini. (2004). "Land Surface Temperature Retrieval from LANDSAT TM 5." *Remote Sensing of Environment* 90 (4): 434–40. https://doi.org/10.1016/J.RSE.2004.02.003.

Sprintall, J., Wijffels, S. and Barker, P. (2002). Ocean surface temperature variability from TOPEX/Poseidon altimetry. Journal of Geophysical Research, 107(C5), 3015.

SPSS, IBM. n.d. "IBM Knowledge Center." Accessed June 13, 2019. https://www.ibm.com/support/knowledgecenter/en/SSLVMB_25.0.0/statistics_mainhelp_ddita/spss/glm/idh_idd_mlp_architecture.html#idh_idd_mlp_architecture.

Srivastava, P.K., Majumdar, T.J. and Amit, K. Bhattacharya. (2009). "Surface Temperature Estimation in Singhbhum Shear Zone of India Using Landsat-7 ETM+ Thermal Infrared Data." *Advances in Space Research* 43 (10): 1563–74. https://doi.org/10.1016/J.ASR.2009.01.023.

Thiemann, Sabine, and Helmut Schiller. (2003). "Determination of the Bulk Temperature from NOAA/AVHRR Satellite Data in a Midlatitude Lake." *International Journal of Applied Earth Observation and Geoinformation* 4 (4): 339–49. https://doi.org/10.1016/S0303-2434(03)00021-7.

Thiemann, S. and Schiller, H. (2003). Remote sensing of ocean colour: An introduction. Journal of Marine Systems, 42(1-2), 1-38.

Threlkeld, Stephen, T. (1990). "Reservoir Limnology; Ecological Perspectives (K. W. Thornton. B.L. Kimmel, and F. E. Payne [Eds.])." *Limnology and Oceanography* 35 (6): 1411–12. https://doi.org/10.4319/lo.1990.35.6.1411.

Wukelic, G.E., Gibbons, D.E., Martucci, I.M. and Foote, H.P. Radiometric calibration of Landsat thematic mapper thermal band. Remote Sensing of Environment 28, 339–347, 1989.

Yang, J, J Qiu - Scientia AAtmosphericSinica, and undefined 1996. n.d. "The Empirical Expressions of the Relation between Precipitable Water and Ground Water Vapor Pressure for Some Areas in China." *Kexue Chubanshe*.

Yokoyama, R., Tanba, S. and Souma. T. (1995). "Sea Surface Effects on the Sea Surface Temperature Estimation by Remote Sensing." International Journal of Remote Sensing 16 (2): 227–38. https://doi.org/10.1080/01431169508954392.

Yokoyama, Y., Tanba, K. and Souma, K. (1995). Remote sensing of sea surface temperature using microwave radiometry. Journal of Geophysical Research, 100(C2), 2353-2362.